World Conference on Timber Engineering Oslo 2023

A SEISMIC RESPONSE ESTIMATION MODEL FOR CROSS-LAMINATED TIMBER WALLS USING MACHINE LEARNING

Eknara Junda[1], Christian Málaga-Chuquitaype[2]

ABSTRACT: This paper proposes a machine learning-based model for estimating the seismic damage of cross-laminated timber (CLT) walls. Random Forests are used to this end. A database is created using numerical results from nonlinear response history analyses under a large set of ground motions. 69 numerical models of CLT walls with various structural characteristics and design parameters are used. The maximum inter-storey drift ratio (MIDR), which plays an essential role in explaining the seismic damage of buildings, is adopted as the damage predictor target. Two feature selection techniques, sequential forward floating selection and LASSO are applied to evaluate the impact of various input features on the estimation performance. Results show that a high accuracy of the estimation is obtained if six features are employed as inputs. The proposed model performance is assessed and then compared with traditional methods. Finally, the Shapley Additive exPlanation method is employed to interpret the influence of the input features on the MIDR estimates in the machine-learning-based model.

KEYWORDS: Seismic demand estimation, Machine learning, CLT walls, Random Forests, Maximum inter-storey drift ratio

1 INTRODUCTION

Cross-laminated timber (CLT) is an environmentally friendly material that offers several advantages in construction, such as high prefabrication level, good thermal insulation, lightweight, and good fire performance when properly designed. CLT has enhanced mechanical properties springing from its manufacturing process resulting in high in-plane strength and stiffness. Thus, CLT has been widely used for walls as the load-bearing element of CLT buildings, including being considered as the lateral force-resisting system in seismic applications [1].

The advantageous mechanical and environmental characteristics of CLT have made it an attractive option for mid to high-rise buildings in earthquake-prone regions. Typical CLT buildings generally comprise panels linked by metal connectors such as hold-downs, angle brackets, and screws. These connectors play a vital role in dissipating the seismic energy through the nonlinear deformation under seismic actions. On the other hand, the CLT panel is assumed to behave as a rigid body [2]. This causes the lateral deformation of CLT buildings to be fundamentally based on a combination of rocking and sliding responses which are completely different from other structural systems, such as moment frames or braced frames governed by flexural behaviour. Such rocking and sliding deformation of CLT walls are complex and challenging to predict due to the overlying effects of pinching, friction, stiffness and strength degradation phenomena. These complex phenomena could also result in high inelastic deformations under strong earthquakes. All this in the context of the continuous push towards taller CLT buildings driven by current developments in construction technology. Therefore, more complex structural behaviours and high seismic demands are expected. Hence, an accurate tool for estimating and assessing the seismic demands of CLT walls is needed.

Seismic demand estimation using machine learning (ML) have increasingly been applied to various structural systems. As ML algorithms do not need functional forms to predict a target, they can successfully map the complex relations between inputs and the target by learning directly from a given dataset. Such abilities to learn and recognise data patterns make ML beneficial for dealing with high-dimensional spaces [3]. ML models for the estimation of seismically-induced responses have been developed for a variety of systems, from geotechnical structures [4] to extra-terrestrial constructions [5]. Likewise, several ML techniques were used to establish regression-based and classification-based models for reinforced concrete [6] and steel frames [7]. ML techniques were also used for other structural systems in the past few years [8-10]. Even though ML techniques have been used for the seismic response estimation of various structural systems, no previous study has applied such techniques to CLT walls. This despite the fact that, as mentioned earlier regarding the complexity of the seismic response of CLT walls, ML techniques have inherent advantages in handling the highly nonlinear

[1] Eknara Junda, Imperial College London, UK, eknara.junda19@imperial.ac.uk
[2] Christian Málaga-Chuquitaype, Imperial College London, UK, c.malaga@imperial.ac.uk

https://doi.org/10.52202/069179-0294

responses and explore the complex relations among parameters of multi-storey CLT walls.

This paper proposes a ML model for estimating the seismic response of multi-storey CLT walls. The maximum inter-storey drift ratio (MIDR) is chosen as the output target. Thirty input features are used as predictors. These features are composed of intensity measures (IMs) and structural parameters of CLT walls (SPs). Sixty-nine numerical models of CLT wall cases with different structural configurations are created and analysed using nonlinear response history analyses to obtain MIDR. Random Forests, a ML algorithm, is used to develop a regression model for MIDR estimates. Finally, the prediction performance of the ML-based models are evaluated and compared with traditional methods. In addition, the influence of each input features on the MIDR prediction is interpreted using SHAP.

2 CLT STRUCTURAL MODELS AND GROUND MOTIONS

2.1 CLT WALL MODELS

69 CLT structures representing residential multi-storey CLT buildings of different heights and panel fragmentation levels are considered. All buildings share the same plan layout and have a typical storey height of 3.5 m, except for the ground level which height is 4.3 m. Figure 1 shows the configuration of a typical 12-storey CLT building as an example. Dead loads were calculated considering all finishing and insulation, whereas a superimposed load of 2.0 kN/m^2 was assumed. Loads considered for seismic mass are a combination of 100% dead and 30% superimposed load. The response spectrum of Eurocode 8 Type 1 [11,12] at a Peak Ground Acceleration (PGA) of 3.0 m/s^2 with an importance factor of 1.0 was adopted to estimate the seismic load.

In this study, CLT Wall 2-BC was selected as the representative part of the structure. The wall is 8.5 m long (marked with dashed lines in Figure 1). All walls were designed using capacity design principles and current codified guidance. We followed ductile design and failure mode control principles informed by Eurocode 8, Part 1. More details of the design processes of the CLT structure can be found in [12].

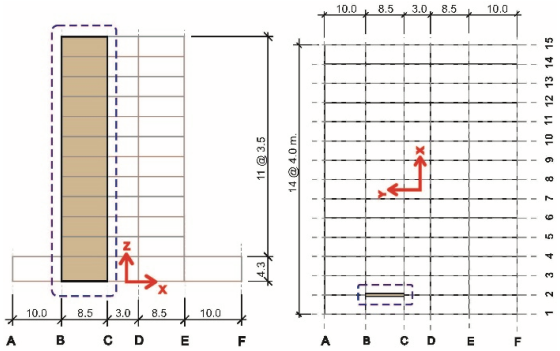

Figure 1: *Typical 12-storey building.*

Several parameters were varied during the design to cover a wide range of CLT buildings and evaluate their effects on the corresponding seismic demands. These parameters comprised the number of storeys, the sub-panel numbers, and the behaviour factors. Table 1 summarises parameters regarding CLT walls adopted in this study.

Table 1: *parameters regarding CLT walls*

Parameters	Variables
Number of stories (N)	6, 8, 12, 16, 20
Number of subpanels per wall (m)	1, 2, 3, 4
Behaviour factor (q)	1.5, 2, 2.5, 3, 4

We developed a series of 2D numerical models of the wall structures in OpenSees [13]. Figure 2 shows a schematic drawing of the model for a wall with m = 2. All CLT panels were discretised into a number of shell elements. In contrast, two-node link elements with zero length represented the three main steel connectors (hold-downs, shear brackets, and vertical screws). The link elements for hold-downs were located at the corners of the panels, represented by blue springs. Angle brackets were distributed along the length of the panels in the X direction (red springs), and self-threaded screws at the vertical joints were lumped into an equivalent single link element, placed at the mid-height of the panels (shown in green).

Since most of the nonlinear deformations in CLT walls under lateral actions occur at their joints and since the CLT panels themselves are expected to remain largely elastic [12,14], an equivalent isotropic material model with linear elastic properties was assumed for the CLT panels. In steel connectors, we used a hysteretic uniaxial material model to capture the global nonlinear responses. Both shear and axial direction capacities were modelled in all types of connectors, considering the uncoupled reaction between the two directions. The strength, deformation values, pinching, strength and stiffness degradation were calibrated against available data from previous experimental studies [15-17]. Moreover, a leaning column, modelled using beam-column elements, was connected to the wall through equal degree-of-freedom constraints to account for P-Delta effects caused by gravity loads. This was done to consider geometric nonlinear effects since the shell element type used in OpenSees only allows for a linear geometric transformation. A Rayleigh damping model with a damping ratio of 0.05 in the first and fifth mode was assumed in all cases.

https://doi.org/10.52202/069179-0294

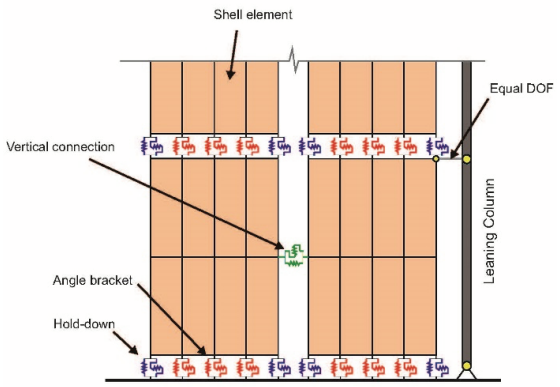

Figure 2: *Numerical model of CLT walls.*

The CLT-walled models mentioned above were validated against experimental results. Two cases of structures, single wall and couple walls are compared and shown In Figures 3 and 4. It is seen from the comparisons that our modelling approach can efficiently reproduce the experimental hysteretic response of CLT assemblages.

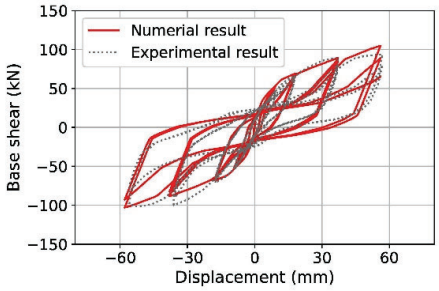

Figure 3: *Validation of the numerical model for a single wall.*

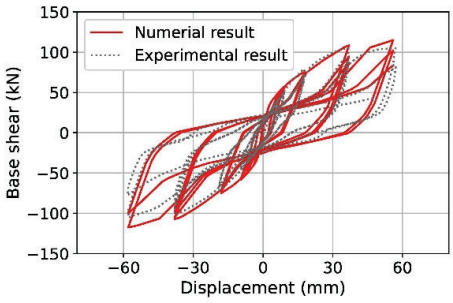

Figure 4: *Validation of the numerical model for coupled walls.*

2.2 GROUND MOTIONS

In this study, we used the 1,656 records selected by Hancock et al. [18] from the NGA-West database [19]. These records come from shallow crust seismic events with moment magnitudes between 5.1 and 7.9 and an average PGA of 1 g. More information regarding the ground motion set can be found in [18]. Moreover, scaling factors of 2 and 1 were used to scale up the original un-scaled records in order to increase the intensity of the ground motions, resulting in more cases of nonlinear responses. Therefore, the total number of ground motion records was 3,312 leading to 228,528 nonlinear response history analyses (NRHA). The massive analysis was performed on the high-performance computing facility (HPC) at Imperial College London.

3 FEATURE SELECTION

To develop an ML model for MIDR estimation, a training dataset was prepared. The dataset consists of the input features (predictors) and the output target (MIDR). Two main parameters were considered for the model development: ground-motion intensity measures (IMs) that describe earthquake characteristics and structural parameters (SPs) that describe structural properties in CLT walls. Nine common IMs were selected based on hazard computability, including Peak Ground Acceleration (PGA), Peak Ground Velocity (PGV), Peak Ground Displacement (PGD), total Arias intensity at the end of the time series (I_a), significant duration ($D_{5–75}$ and $D_{5–95}$), and spectral acceleration values at the building's fundamental period ($S_a(T_1)$) and at n times T_1 ($S_a(nT_1)$) where n was varied from 1.1 to 3.0, the mean period of the ground motion (T_m) and the ratio between the fundamental structural period and the ground-motion mean period (the tuning ratio, T_1/T_m). In addition, six structural parameters (SPs) were also considered as candidate input features. These include the behaviour factor (q), building height (H), slenderness (λ_w), length of fastening lines (FL), joint density (β_w), and wall subdivision ratio (m). These SPs have been reported in the literature to significantly impact the seismic response of CLT wall structures [14, 20, 21]. The total number of input features was 30.

We randomly divided the whole database into training and test sets to avoid overfitting during the model development. The training set contained 70 % of the database and was used for all the activities of the modelling processes, whereas the remaining 30 % of the data was kept as unseen data and was used for performance testing purposes at the final step. We transformed all IMs and MIDR to the log-normal space following the common assumption of lognormality adopted in earthquake engineering [22].

All 30 input features used for the model development were selected using different feature selection techniques, namely sequential forward floating selection (SFFS) and Least Absolute Shrinkage and Selection Operator (LASSO). The feature selection was carried out using the training dataset. Note that the objective of this process is to evaluate the predictive potential of the features and obtain a set of features influencing the prediction. The mean square error (MSE) was used to assess the fit, and a 10-fold cross-validation (CV) was applied to generalise the results, mitigate overfitting, and improve the model's robustness [23]. The features which finally selected were PGV, $S_a(T_s)$, T_1/T_m, q, H, and m. This set was considered

https://doi.org/10.52202/069179-0294

as an optimised combination of predictors, which was used to develop the ML model in this paper.

4 MACHINE LEARNING MODEL DEVELOPMENT

4.1 MODEL TRAINING

As mentioned previously, this paper compares the performance of MIDR estimates between a traditional regression model and an ML-based model. The algorithm used for a traditional method is Multiple Linear Regression, whereas an ML method is Random Forest. We have implemented the algorithms using the Scikit-learn package in the Python-based computational platform. Note that hyper-parameters of Random Forest were tuned to minimise a cost function using GridSearchCV, also available from the Scikit-learn package.

4.2 PERFORMANCE MEASURES

This study employs two performance metrics, the coefficient of determination (R^2) and the root mean square error (RMSE), to assess the applied models' prediction performance. These two indicators, widely adopted in ML performance studies, are provided for training and test sets. The expressions for R^2 and RMSE are given in Equations 1 and 2.

$$R^2 = 1 - \frac{\sum_{i=1}^{n}(y_i - \hat{y}_i)^2}{\sum_{i=1}^{n}(y_i - \bar{y}_i)} \quad (1)$$

$$RMSE = \sqrt{\frac{1}{n}\sum_{i=1}^{n}(y_i - \hat{y}_i)^2} \quad (2)$$

where $\hat{y}_i$is the estimated target out, $y_i$is the real target value, and n is the number of data points.

5 RESULTS

5.1 MODEL PERFORMANCES

The prediction performances of the training and test datasets for the regression models are presented in Table 2. The MIDR estimates versus actual values are depicted in Figures 5 and 6 for the linear regression and random forest models, respectively. The result shows a comparable prediction performance between the training and the test set. This indicates that the models developed do not overfit the training data and should perform well on unseen data.

Table 2: *Comparison of the prediction performances*

Algorithm	MIDR			
	Training set		Test set	
	R^2	RMSE	R^2	RMSE
Linear regression	0.778	0.368	0.777	0.369
Random Forest	0.950	0.102	0.946	0.198

The traditional linear regression, which has been broadly applied for estimating seismic demands of structures, shows relatively low prediction power, evidenced by the lower R^2 and higher values of RMSE, compared to the Random Forest. The linear regression model clearly has notable dispersion levels between its predictions and numerical results, especially underestimating MIDRs at higher levels of demand. Lower performances are observed from the linear regression with R^2 of 0.777 and RMSE of 0.369 on the test set for MIDR estimates. This indicates that traditional approaches like Linear Regression might not be able to predict MIDR over the full range of deformation in CLT structures. The low prediction performances can be partially attributed to its inability to describe highly nonlinear processes and complex relationships between the input features and MIDRs. On the other hand, the model developed from Random Forest shows substantial improvements in prediction power over the traditional method, reflected by 21.75% higher values of R^2 and 46.34% lower values of RMSE. The results clearly show that Random Forest can capture better the non-linearity in the drift response of CLT walls.

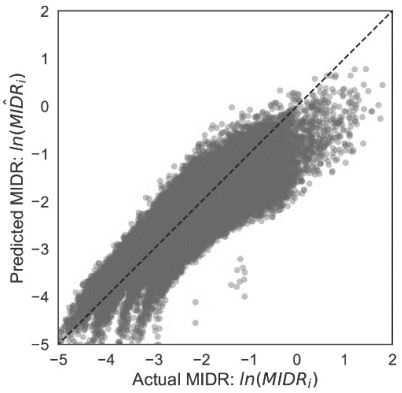

Figure 5: *Comparison between actual and predicted MIDR from the Linear Regression model.*

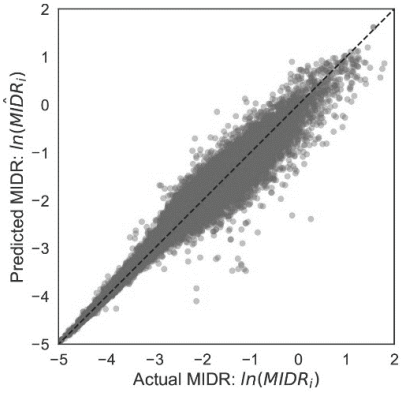

Figure 6: *Comparison between actual and predicted MIDR from the Random Forest model.*

https://doi.org/10.52202/069179-0294

5.2 MODEL INTERPRETATION

Machine learning models can be difficult to understand and are sometimes seen as black boxes due to their complex algorithms. It is essential to know how a model makes predictions and which factors affect the model. To this end, SHAP methodology [24] was used to explain our ML model, Random Forest. Figure 7 shows the SHAP summary plot for MIDR. Each point in this graph shows the relation between the six features and the SHAP value obtained from the Random Forest model. The features are ordered from top to bottom based on their overall importance to the model prediction. It is observed that $\ln(S_a(T_1))$ is the most important feature, followed by H, ln(PGV), m, q, and $\ln(T_1/T_m)$. The variation in colours, from blue to red, represents the variation of the features from low to high, respectively. Moreover, data points that result in the same SHAP value are scattered, leading to different distribution shapes for the features.

The SHAP summary indicates that MIDR positively corresponds to almost input features except for $\ln(T_1/T_m)$. An increase in SHAP value goes along with an increase in $\ln(S_a(T_1))$, H, ln(PGV), m, and q. In the case of $\ln(T_1/T_m)$, lower values have more impact on MIDR than higher values, as the red dots are concentrated approximately in the SHAP value of 0. It is also observed that small SHAP values (SHAP values < 0) are sensitive to the variation of all features, reflected in the long blue tails to the left. This indicates that all features significantly impact the low range of MIDR, especially in the case of $\ln(S_a(T_1))$. The SHAP explanation is consistent with the fact that this range of MIDR is strongly dependent on the elastic stiffness of the structures, as well as their yield strength and structural configuration. On the other hand, ln(PGV) influences the model for large MIDR values significantly. Other features become progressively less influential on the prediction, especially m, q, and $\ln(T_1/T_m)$.

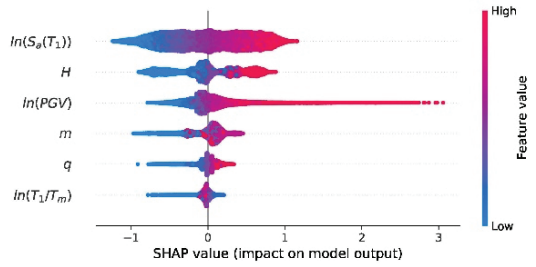

Figure 7: *SHAP summary plots for MIDR.*

Figures 8, 9 and 10 show scatter diagrams displaying local feature importance for the input features and SHAP values. The plots also indicate the interaction between a pair of features considered represented by the transition from blue (low values) to red (high values), as shown on the right of the plots. Overall, it is observed that a highly nonlinear influence of all the IMs examined over the MIDR. $\ln(S_a(T_1))$ and ln(PGV) have a positive relation with MIDR, although they have different trends. This can be explained by the fact that higher values of $\ln(S_a(T_1))$ and ln(PGV) lead to higher SHAP values, which are associated with larger MIDRs. The impact of $\ln(S_a(T_1))$ on the estimation of MIDR decreases moderately, while ln(PGV) tends to increase exponentially.

In the case of $\ln(T_1/T_m)$, a positive impact on the drift estimation is observed until $\ln(T_1/T_m)$ reaches a value of 1. After that, $\ln(T_1/T_m)$ has no impact on the prediction denoted by the almost unchanged SHAP values. This marks an explicit limitation to the predictive power of T_1/T_m that peaks at "resonance" and decays afterwards. This reduction in the predictive ability of T_1/T_m can be partially due to the rise in the importance of structural yielding.

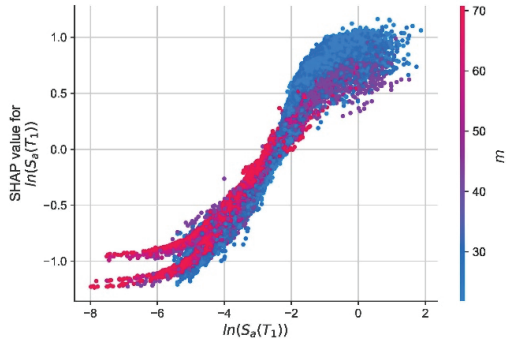

Figure 8: *SHAP dependent plots for MIDR and $\ln(S_a(T_1))$.*

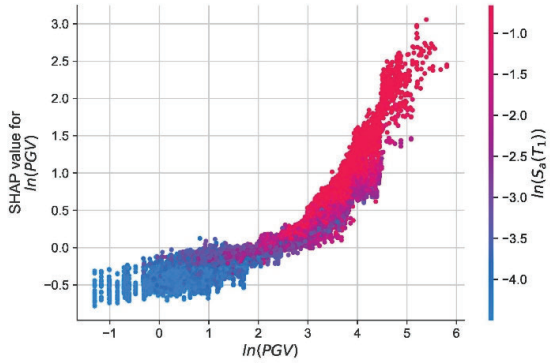

Figure 9: *SHAP-dependent plots for MIDR and ln(PGV).*

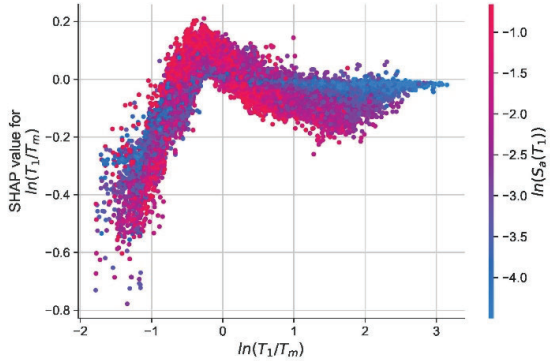

Figure 10: *SHAP-dependent plots for MIDR and $\ln(T_1/T_m)$.*

Figures 11, 12, and 13 depict the SHAP dependency plots for the three structural parameters used to formulate our model. They show that H and q positively impact the MIDR prediction. However, for q values of 3 or larger, MIDR becomes less sensitive to q. On the other hand, the trend of m changes from positive to slightly negative after a value of 3. This suggests that subdividing a CLT wall into more than three sub-panels is unnecessary.

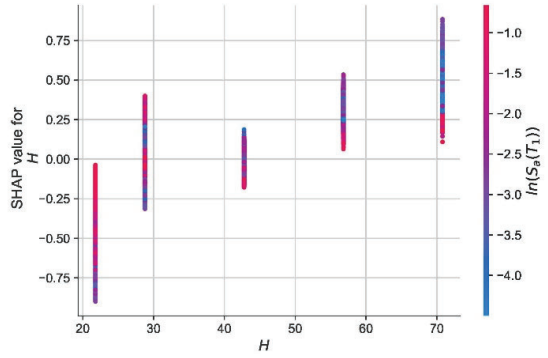

Figure 11: *SHAP-dependent plots for MIDR and H.*

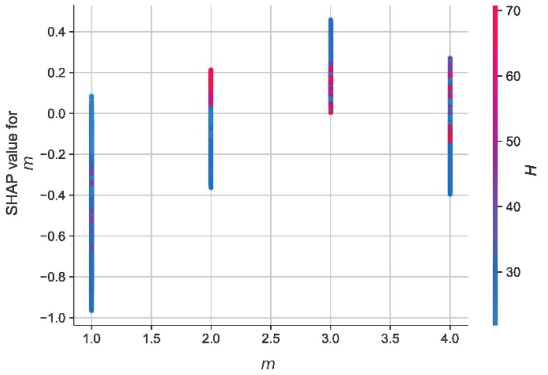

Figure 12: *SHAP-dependent plots for MIDR and m.*

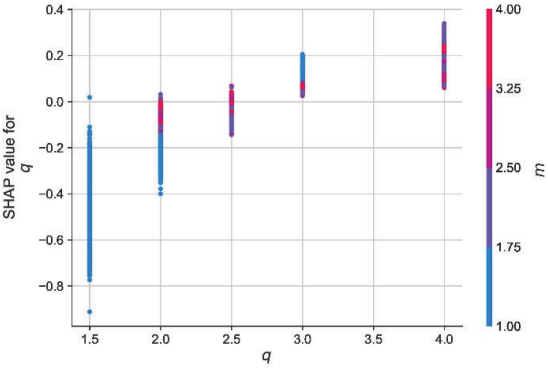

Figure 13: *SHAP-dependent plots for MIDR and q.*

6 CONCLUSION

This paper has investigated the use of machine learning (ML) to estimate the maximum inter-storey drift (MIDR) in multi-story CLT structures and compared it with traditional regression approaches. To do this, we have built numerical models of 69 CLT-walled structures with various structural configurations and design attributes, which reflect a wide variety of CLT building configurations. After calibrating the accuracy of the numerical models against available experimental data, we use them to generate MIDRs of the wall structures using extensive nonlinear response history analyses under a database of 3,312 real ground-motion records scaled with factors of 1.0 and 2.0. The large dataset of seismic drift demands is used as output targets. A total of 30 characteristics, including ground-motion intensity measurements and structural factors, were examined for their influence on the MIDR estimates. Two data-science-based feature selection methods, SFFS and LASSO, are used to inform the suitable set of features to estimate MIDR. A set of six most significant features is obtained, namely the spectral acceleration at T_1 ($S_a(T_1)$), peak ground velocity (PGV), the period ratio (T_1/T_m), behaviour factor (q), structure height (H), and wall ratios (m).

Two regression models are developed and compared with their prediction performances using R^2 and RMSE. The results demonstrate that the traditional linear regression, widely applied for estimating seismic demands of structures, has low prediction power. This indicates that the traditional method oversimplifies the complex nature of the seismic response and cannot provide reliable MIDR estimates over the full range of deformations in CLT structures, but this is especially true at higher deformation levels where the linear model underestimates the drift response. In contrast, the Random Forest model significantly outperforms the traditional method, which is 21.75% higher in R^2 and 46.34% lower in RMSE. The findings show that Random Forest captures better the nonlinearity of MIDR in multi-storey CLT walls.

The SHAP important plots reveal that $S_a(T_1)$ and T_1/T_m strongly influence the drift prediction for tiny drifts where the structure remains elastic while PGV dominates the model at large displacements. The results also imply that a q and an m value of 3 can be optimal for multi-story CLT buildings since an increase in their value beyond those levels will not significantly improve the overall ductility of CLT structures.

REFERENCES

[1] Sullivan K, Miller TH, Gupta R. Behavior of cross-laminated timber diaphragm connections with self-tapping screws. Engineering Structures 2018;168:505–24. https://doi.org/10.1016/j.engstruct.2018.04.094.

[2] Sandoli A, D'Ambra C, Ceraldi C, Calderoni B, Prota A. Sustainable cross-laminated timber structures in a seismic area: Overview and future trends. Applied Sciences (Switzerland) 2021;11:1–24. https://doi.org/10.3390/app11052078.

[3] Málaga-Chuquitaype C. Machine Learning in Structural Design: An Opinionated Review.

https://doi.org/10.52202/069179-0294

Frontiers in Built Environment 2022;8:1–12. https://doi.org/10.3389/fbuil.2022.815717.

[4] Macedo J, Liu C, Soleimani F. Machine-learning-based predictive models for estimating seismically-induced slope displacements. Soil Dynamics and Earthquake Engineering 2021:106795. https://doi.org/10.1016/j.soildyn.2021.106795.

[5] Maqdah J, Memarzadeh M, Kampas G, Málaga-Chuquitaype C. AI-aided exploration of lunar arch forms under in-plane seismic loading. Acta Mechanica 2023. https://doi.org/10.1007/s00707-023-03520-7

[6] Meng X, Shi L, Yao L, Zhang Y, Cui L. Machine learning-based approaches for seismic demand and collapse of ductile reinforced concrete building frames. Colloids and Surfaces A: Physicochemical and Engineering Aspects 2020:124658. https://doi.org/10.1016/j.jobe.2020.101905.

[7] Zahra F, Macedo J, Málaga-Chuquitaype C. Hybrid data-driven hazard-consistent drift models for SMRF. Earthquake Engineering and Structural Dynamics 2023; 52(4):1112-1135. https://doi.org/10.1002/eqe.3807

[8] Wu J, Baker JW. Statistical learning techniques for the estimation of lifeline network performance and retrofit selection. Reliability Engineering and System Safety 2020;200:106921. https://doi.org/10.1016/j.ress.2020.106921.

[9] Ni P, Mangalathu S, Liu K. Enhanced fragility analysis of buried pipelines through Lasso regression. Acta Geotechnica 2020;15:471–87. https://doi.org/10.1007/s11440-018-0719-5.

[10] Mangalathu S, Ph D, Asce AM, Jeon J, Ph D. Machine Learning – Based Failure Mode Recognition of Circular Reinforced Concrete Bridge Columns : Comparative Study. Journal of Structural Engineering 2019;145:1–12. https://doi.org/10.1061/(ASCE)ST.1943-541X.0002402.

[11] (CEN) EC for S. Eurocode 8: Design of structures for earthquake resistance-Part 1: General rules, seismic actions and rules for buildings. 2004. https://doi.org/10.1680/cien.2001.144.6.55.

[12] Málaga-Chuquitaype C. Chapter 8: Design of timber structures in Seismic Design of Buildings to Eurocode 8 (CRC Press, 2016), 213–234.

[13] McKenna F. OpenSees: A framework for earthquake engineering simulation. Computing in Science and Engineering 2011;13:58–66. https://doi.org/10.1109/MCSE.2011.66.

[14] Demirci C, Málaga-Chuquitaype C, Macorini L. Seismic drift demands in multi-storey cross-laminated timber buildings. Earthquake Engineering and Structural Dynamics 2018;47:1014–31. https://doi.org/10.1002/eqe.3003.

[15] Gavric I, Fragiacomo M, Ceccotti A. Cyclic behaviour of typical metal connectors for cross-laminated (CLT) structures. Materials and Structures/Materiaux et Constructions 2015;48:1841–57. https://doi.org/10.1617/s11527-014-0278-7.

[16] Gavric I, Fragiacomo M, Ceccotti A. Cyclic behaviour of typical screwed connections for cross-laminated (CLT) structures 2015:179–91. https://doi.org/10.1007/s00107-014-0877-6.

[17] Gavric I, Fragiacomo M, Ceccotti A. Cyclic behavior of CLT wall systems: Experimental tests and analytical prediction models. Journal of Structural Engineering (United States) 2015;141:1–14. https://doi.org/10.1061/(ASCE)ST.1943-541X.0001246.

[18] Hancock J, Bommer JJ, Stafford PJ. Numbers of scaled and matched accelerograms required for inelastic dynamic analyses. Earthquake Engineering & Structural Dynamics 2008:1585–607. https://doi.org/10.1002/eqe.

[19] Campbell KW, Eeri M, Bozorgnia Y, Eeri M. NGA Ground Motion Model for the Geometric Mean Horizontal Component of NGA Ground Motion Model for the Geometric Mean Horizontal Component of PGA , PGV , PGD and 5 % Damped Linear Elastic Response Spectra for Periods Ranging from 0 . 01 to 10 s. Earthquake Spectra 2008;24:139–71. https://doi.org/10.1193/1.2857546.

[20] Demirci C, Málaga-Chuquitaype C, Macorini L. Seismic shear and acceleration demands in multi-storey cross-laminated timber buildings. Engineering Structures 2019;198:109467. https://doi.org/10.1016/j.engstruct.2019.109467

[21] Pozza L, Trutalli D. An analytical formulation of q-factor for mid-rise CLT buildings based on parametric numerical analyses. Bulletin of Earthquake Engineering 2017;15:2015–33. https://doi.org/10.1007/s10518-016-0047-9.

[22] Shome N, Cornell CA, Bazzurro P, Carballo JE. Earthquakes, records, and nonlinear responses. Earthquake Spectra 1998;14:469–500.

[23] Kohavi R. A study of cross-validation and bootstrap for accuracy estimation and model selection. Ijcai, vol. 14, Montreal, Canada; 1995, p. 1137–45.

[24] Liu GR. Interpretable Machine Learning with Python. 2022. https://doi.org/10.1142/12774.